Proton irradiation effects on minority carrier diffusion length and defect introduction in homoepitaxial and heteroepitaxial n-GaN

K. C. Collins,[1,a)] A. M. Armstrong,[2,a)] A. A. Allerman,[2] G. Vizkelethy,[2] S. B. Van Deusen,[2] F. Léonard,[1] and A. A. Talin[1,b)]
[1]*Sandia National Laboratories, 7011 East Ave., Livermore, California 94550, USA*
[2]*Sandia National Laboratories, 1515 Eubank, SE, Albuquerque, New Mexico 87123, USA*

(Received 27 September 2017; accepted 30 November 2017; published online 21 December 2017)

Inherent advantages of wide bandgap materials make GaN-based devices attractive for power electronics and applications in radiation environments. Recent advances in the availability of wafer-scale, bulk GaN substrates have enabled the production of high quality, low defect density GaN devices, but fundamental studies of carrier transport and radiation hardness in such devices are lacking. Here, we report measurements of the hole diffusion length in low threading dislocation density (TDD), homoepitaxial n-GaN, and high TDD heteroepitaxial n-GaN Schottky diodes before and after irradiation with 2.5 MeV protons at fluences of 4–6 $\times 10^{13}$ protons/cm^2. We also characterize the specimens before and after irradiation using electron beam-induced-current (EBIC) imaging, cathodoluminescence, deep level optical spectroscopy (DLOS), steady-state photocapacitance, and lighted capacitance-voltage (LCV) techniques. We observe a substantial reduction in the hole diffusion length following irradiation (50%–55%) and the introduction of electrically active defects which could be attributed to gallium vacancies and associated complexes (V_{Ga}-related), carbon impurities (C-related), and gallium interstitials (Ga_i). EBIC imaging suggests long-range migration and clustering of radiation-induced point defects over distances of ~500 nm, which suggests mobile Ga_i. Following irradiation, DLOS and LCV reveal the introduction of a prominent optical energy level at 1.9 eV below the conduction band edge, consistent with the introduction of Ga_i. *Published by AIP Publishing.* https://doi.org/10.1063/1.5006814

I. INTRODUCTION

The recent commercial availability of free-standing, bulk GaN substrates with a thickness of several hundred microns and dislocation densities $<10^6$ cm^{-2} has spurred strong interest in vertical GaN-based diodes and transistors for high power applications.[1] The high critical field strength of GaN allows for a reduction in the thickness of the drift region in power devices, thus reducing the "ON" state resistance. The high carrier mobility of GaN further improves the device power performance, as summarized by Baliga's figure of merit: $BFOM = \varepsilon\mu E_G{}^3$, where ε is the dielectric constant, μ is the mobility, and E_G is the bandgap of the semiconductor.[2] For high power unipolar devices, GaN can theoretically outperform SiC.[3] Additionally, stronger atomic bonding leads to the superior radiation hardness of GaN compared to Si and GaAs,[4] making GaN devices attractive for space-based and other applications with potentially high radiation exposure. In the past, a lack of native substrates required heteroepitaxial GaN growth on sapphire, Si, and SiC, resulting in threading dislocation densities (TDDs) of ~10^8 cm^{-2} or more.[1] Dislocations and point defects degrade device performance by acting as traps and recombination centers which lower minority carrier lifetime and mobility. Recent progress in the hydride vapor phase epitaxy (HVPE) growth of bulk, free-standing GaN[5–7] has achieved large (2 in. diameter) GaN substrates with TDDs of ~10^6 cm^{-2} or less, suitable for the epitaxial growth of low dislocation density GaN active device layers.

Energetic radiation in the form of neutrons, protons, and electrons damages the GaN lattice by producing defects that act as minority carrier traps and recombination centers.[8] In general, the extent of the damage depends strongly on the type of particle, the fluence, and the energy. Proton irradiation and electron irradiation with MeV energies primarily introduce point defects in GaN.[4,8] Prior studies on proton radiation effects on GaN grown on sapphire or SiC substrates (TDDs ~ 10^8 cm^{-2} or more) found substantial decreases in minority carrier diffusion lengths and lifetimes in n-GaN and p-GaN.[9–12] We recently reported the effect of radiation on the carrier diffusion length in low defect density GaN grown on a free-standing GaN substrate, finding that 2.5 MeV protons at a fluence of 4 $\times$ 10^{13} protons/cm^2 decreased the hole diffusion length by 55%.[13] Here, we expand upon that result with a comparison to high TDD GaN and a more detailed examination of the radiation-introduced defects.

In this manuscript, we compare the effects of 2.5 MeV proton irradiation with fluences of 4–6 $\times 10^{13}$ protons/cm^2 on the hole diffusion length in low TDD (~1×10^6 cm^{-2}) GaN grown by metal organic chemical vapor deposition (MOCVD) on commercially available free-standing, HVPE-grown GaN substrates and on high TDD (~2.6×10^8 cm^{-2}) GaN grown by MOCVD on (0001) sapphire substrates. We use electron beam-induced-current (EBIC) in a depth-dependent configuration[14] to measure hole diffusion lengths. We also compare

[a)]K. C. Collins and A. M. Armstrong contributed equally to this work.
[b)]Author to whom correspondence should be addressed: aatalin@sandia.gov

defect concentrations in the pre- and post-radiation samples using EBIC imaging, cathodoluminescence (CL), deep level optical spectroscopy (DLOS), steady-state photocapacitance (SSPC), and lighted capacitance-voltage (LCV). We find that radiation substantially lowers hole diffusion lengths in both high and low TDD GaN and introduces electrically and optically active point defects, including long-range, room temperature point defect segregation.

II. SAMPLE PREPARATION

Si-doped, n-type GaN was grown by MOVCD on two commercially available GaN substrates: an HVPE-grown, free-standing GaN substrate with low dislocation density ($\sim 10^6\,cm^{-2}$), which we refer to as low TDD GaN, and a GaN-on-sapphire template with higher dislocation density GaN ($\sim 10^8\,cm^{-2}$), resulting in a GaN layer with a dislocation density of $\sim 2.6 \times 10^8\,cm^{-2}$, estimated from EBIC imaging, which we refer to as high TDD GaN. The low TDD GaN epilayers have a net doping, $N_d \sim 1 \times 10^{16}\,cm^{-3}$, and a thickness of 8 μm, while the high TDD epilayer has $N_d \sim 3 \times 10^{16}\,cm^{-3}$ and a thickness of 1.3 μm. To facilitate measurements, an array of thin Schottky contacts (~10–15 nm thick) was formed by evaporating Ni through a shadow mask, and In was used to form ohmic contacts.

A portion of each wafer was irradiated with 2.5 MeV protons at the Ion Beam Laboratory at Sandia National Laboratories. A spatially uniform exposure over the device area was used, devices were unbiased during the irradiation, and no post-radiation annealing was performed. The low TDD material was irradiated with a fluence of 4×10^{13} protons/cm^2, and the high TDD material was irradiated with a fluence of 6×10^{13} protons/cm^2. Both irradiated and unirradiated materials were subsequently examined with a variety of methods, as described below. As shown in Sec. IV, the deep level defect introduction rate and thus the expected carrier removal rate were $\sim 100\,cm^{-1}$ for both samples. The reduction in free carrier density due to irradiation was then $\sim 5 \times 10^{15}\,cm^{-3}$ for both samples, which was much less than the original net doping density.

III. DIFFUSION LENGTH MEASUREMENTS WITH EBIC

Electron beam-induced-current (EBIC) is a commonly used technique to measure the minority carrier diffusion length in semiconductors. EBIC uses an electron beam (e-beam) in a SEM to excite electron hole pairs (e-h pairs) in a semiconductor near a space-charge region (SCR), where the pairs can be separated and collected. The resulting current is measured as the e-beam distance to the SCR is varied, providing information on the diffusion length of minority carriers, $L = (D\tau)^{1/2}$, where D is the diffusivity and τ is the carrier lifetime.

In a recent report, Yakimov pointed out the common pitfalls when using EBIC to measure relatively short L ($\lesssim 1\,\mu$m), as is typically the case with GaN.[14] Yakimov suggested that a depth-dependent configuration is more accurate, compared to the commonly used planar-collector configuration, for the case when the e-h pair generation volume produced by the primary e-beam is comparable to or larger than the SCR. Figure 1(a) illustrates three EBIC configurations for measuring L: planar-collector, normal-collector, and depth-dependent.[15] In the planar-collector and normal-collector configurations, the e-h pair injection distance from the edge of a SCR is varied by scanning the e-beam. The normal-collector configuration is more challenging to implement, requiring cleaving of the sample through the junction, and so, planar-collector configurations are more commonly used. However, the simple model for evaluating planar-collector data relies on several assumptions which are difficult to satisfy when L is small.[14] In particular, the distance from the injection point to the edge of the SCR, d, must be much larger than the size of the e-h pair generation volume, R. At an e-beam accelerating voltage of 15 keV, R in GaN is ~800 nm.[16] For $L < 1\,\mu$m, collecting an EBIC signal for $d \gg R$ is challenging due to the small signal to noise ratio. The depth-dependent approach suggested by Yakimov relies on the injection of e-h pairs below the SCR through the contact and varies the injection depth by changing the e-beam accelerating voltage.

Literature reports for GaN diffusion lengths show wide variability, which can be attributed in part to the particular EBIC configuration used. Figure 1(b) shows reported hole diffusion lengths in n-GaN (L_h) versus dislocation density

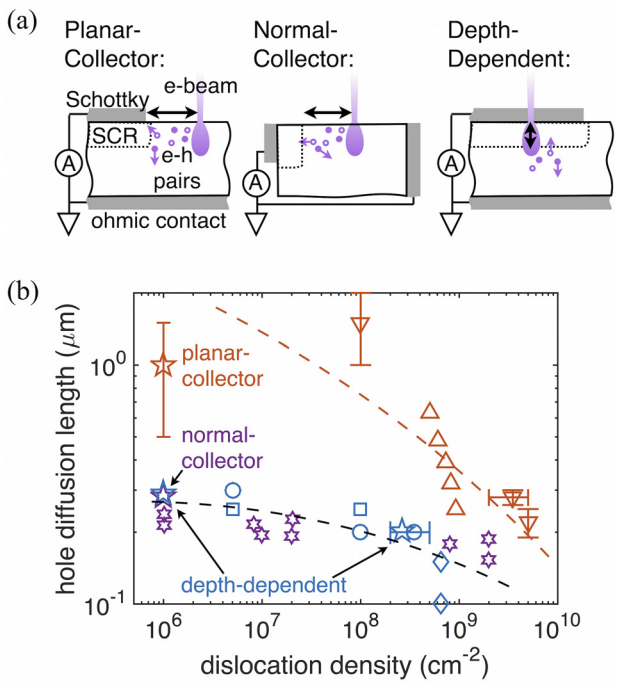

FIG. 1. (a) Schematic of the three EBIC configurations used for measuring the minority carrier diffusion length. (b) Reported values for the hole diffusion length in unirradiated n-GaN vs. dislocation density, acquired using the planar-collector (red), normal collector (purple), or depth-dependent (blue) configurations. Measurements from this work on unirradiated GaN with low and high defect densities are included (pentagrams). The same low dislocation density sample was measured using all three EBIC configurations, and good agreement was found between normal-collector and depth-dependent data, while planar-collector data give much higher diffusion length values. Dashed lines are a guide to the eye. Planar-collector literature data from Ref. 17 (downward triangles) and Ref. 18 (upward triangles), normal-collector literature data from Ref. 19 (hexagrams), and depth-dependent literature data from Ref. 20 (circles), Ref. 21 (squares), and Ref. 22 (diamonds) are shown.

and distinguishes between the three EBIC experimental configurations discussed above. Good agreement is apparent between the data from normal-collector and depth-dependent configurations, while planar-collector measurements are outliers with much higher L_h values. We verified this trend by measuring L_h on the same unirradiated, low TDD n-GaN sample using all three EBIC configurations [Fig. 1(b)]. We found excellent agreement between our depth-dependent and normal-collector measurements, while the planar-collector yielded significantly larger L_h values that varied widely with accelerating voltage. Based on this result and the arguments made by Yakimov, we choose to use the depth-dependent configuration for our radiation study.

We use depth-dependent EBIC to measure the diffusion length, averaging data for 3–5 Schottky diodes over a wafer area of a few mm^2 to account for material variations. Accelerating voltages from 3 to 30 keV or 3–18 keV were used for the low and high TDD diodes, respectively, corresponding to electron ranges of ~50 nm–2.7 μm or ~50 nm–1.1 μm,[16] and no bias was applied. Figure 2 shows the averaged measured hole diffusion lengths for low and high TDD GaN as a function of proton fluence. Both low and high TDD GaN exhibit large declines in L_h following irradiation (50%–55%), equivalent to a ~4–5× increase in point defect density due to irradiation, assuming $L_h \propto {N_D}^{-1/2}$, where N_D is the density of point defects. High TDD GaN showed a more modest decline in the diffusion length compared to low TDD GaN. TDDs may getter point defects, mitigating the effects of irradiation on the diffusion length to some degree.

IV. DEFECT CHARACTERIZATION

We examine the defects introduced by proton irradiation using a variety of methods, including EBIC imaging, cathodoluminescence (CL), deep level optical spectroscopy (DLOS), steady-state photocapacitance (SSPC), and lighted capacitance-voltage (LCV). The results from each method are presented below.

A. EBIC imaging of defects

EBIC images of low and high TDD GaN, both before and after irradiation, are shown in Fig. 3. The images were collected by injecting carriers through the thin Ni Schottky contacts using an accelerating voltage of 10 kV, which corresponds to an electron range of ~400 nm.[16] Before irradiation, the low TDD GaN shows very little contrast [see Fig. 3(a)], while the high TDD GaN has a series of dark spots that are generally associated with TDs [see Fig. 3(c)]. TDs act as traps and recombination centers, leading to lower EBIC when carriers are injected nearby.

Following irradiation, the overall EBIC magnitude declines for both low and high TDD GaN, suggesting the introduction of a measurable density of electronically active defects. Interestingly, in addition to a decrease in the overall EBIC signal, we also observe a subtle pattern emerging in the EBIC contrast in irradiated samples [see Figs. 3(b) and 3(d)]. Similar EBIC contrast patterns have been observed following proton irradiation of GaAs.[23,24] Proton irradiation at 2.5 MeV primarily introduces point defects in GaN,[8] which are too small to be individually resolved with EBIC. The irradiation conditions should have produced a uniform distribution of point defects over the specimen dimensions (~0.5 cm^2). The stopping depth for 2.5 MeV protons in our devices is calculated to be >30 μm,[25] well below the examined depth. Furthermore, the irradiation was done with a uniform exposure, and no post-radiation annealing was performed. The EBIC pattern we observe suggests that point defects migrate and cluster in GaN at room temperature. Internal strain in the GaN layer may provide a driving force for point defect migration.

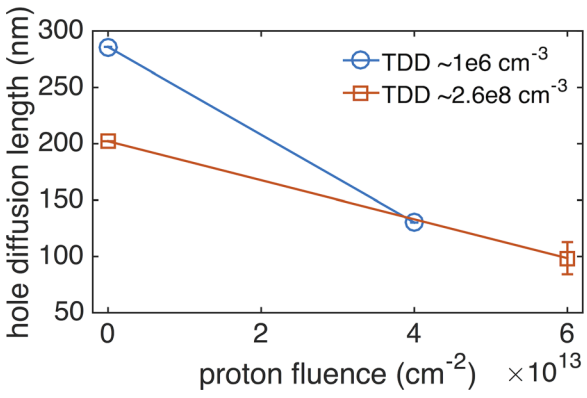

FIG. 2. Measured hole diffusion lengths in low and high TDD GaN following irradiation with 2.5 MeV protons.

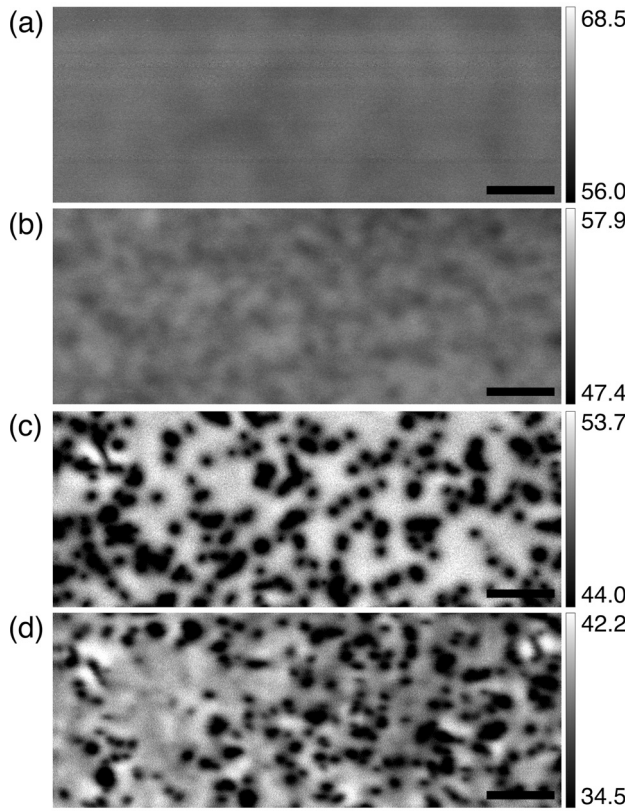

FIG. 3. EBIC images of low TDD GaN as-grown (a) and irradiated with 4 × 10^{13} protons/cm^2 (b) and high TDD GaN as-grown (c) and irradiated with 6 × 10^{13} protons/cm^2 (d). The scale bar is all 2 μm. Color bars show EBIC magnitudes in nA. For ease of comparison, the maximum color bar range was chosen to span ±10% about the mean EBIC value.

Prior studies have suggested that gallium interstitials (Ga_i) are mobile at room temperature. Using optically detected paramagnetic resonance in photoluminescence, Chow *et al.* found that 2.5 MeV electron irradiation introduced a defect that could be identified as Ga_i and observed that these became mobile at temperatures slightly below room temperature.[26] First-principles calculations by Limpijumnong and Van de Walle determined the formation and migration energies for interstitial and vacancy defects in GaN, finding that Ga_i has a relatively low migration barrier ($E_m \leq 0.9$ eV).[27] To generate the EBIC patterns we observe, which have an average feature size of $\sim 1\,\mu$m, point defects would have to migrate ~ 500 nm at room temperature. Assuming thermally activated migration, we can estimate the diffusivity as $D = D_o exp(-E_m/k_B T)$, where E_m is the migration energy barrier, T is temperature, and k_B is Boltzmann's constant. An experimental study of nitrogen self-diffusion in $Ga^{15}N/Ga^{14}N$ heterostructures found $D_o = 1600\,cm^2/s$.[28] Assuming $E_m = 0.9$ eV and $D_o = 1600\,cm^2/s$ to obtain an order of magnitude estimation, we approximate a room temperature diffusivity of $D \approx 1.2 \times 10^{-12}$ cm^2/s, suggesting that Ga_i point defects could diffuse a distance of $L \approx 500$ nm in $t \approx 35$ min ($L = (Dt)^{0.5}$). Our EBIC measurements were performed weeks after GaN layer growth and irradiation, providing ample time for migration. Notably, based on Limpijumnong and Van de Walle's calculations, Ga_i are the only point defects that are sufficiently mobile at room temperature, with nitrogen interstitials (N_i) having the next lowest migration energy barrier of $E_m \approx 1.5$ eV, requiring a temperature of $\sim 200\,^{\circ}C$ to traverse 500 nm in a few hours, suggesting that the EBIC pattern we observe is most likely due to the migration of Ga_i. Furthermore, a prior study of GaN on SiC with high resolution x-ray diffraction observed improved local crystallinity as mobile point defects diffused towards extended defects and determined a point defect diffusion length of ~ 500 nm,[29] in agreement with our findings. Additional studies with high resolution TEM would be needed to confirm that the EBIC contrast formations we observe are indeed clusters of point defects. Nevertheless, our results point to EBIC as a promising method for studying point defect migration in GaN.

B. CL spectra

Cathodoluminescence (CL) spectra help identify optically active defects by revealing their energy within the bandgap and providing an estimate of their relative concentrations. CL spectra before and after proton irradiation are shown in Fig. 4 for both low and high TDD GaN. CL spectra were collected with a 30 keV e-beam accelerating voltage, with the e-beam rastering at TV-mode speeds over a small area of the sample ($\sim 12\ \mu m^2$). For both specimens, we observe a green luminescence band (GL) near 2.47 eV. The CL spectrum for the low TDD specimen also reveals a more pronounced shoulder by the near band edge (NBE) peak and a weak and broad blue level (BL) peak near 2.90 eV. The GL can be associated with gallium vacancies (V_{Ga}) and related complexes, especially with oxygen ($V_{Ga}O_N$), which tends to move the commonly observed yellow band towards the green band.[27,30] Blue bands have also been observed in MOCVD and HPVE-grown GaN and can also be attributed to V_{Ga}-related defects.[30] Following proton irradiation, the CL intensity decreases substantially across all wavelengths, and the BL in the low TDD GaN disappears. Lower CL intensity indicates that radiation-induced damage increases non-radiative recombination rates. Similar CL spectral changes following high fluence proton irradiation have been observed, with lower CL intensities and the disappearance of the blue band.[9] Further analysis of the spectra reveals that the ratio of the integrated intensities GL/NBE increased from 1.1 to 1.5 for the low TDD specimen and from 1.1 to 1.3 for the high TDD specimen.

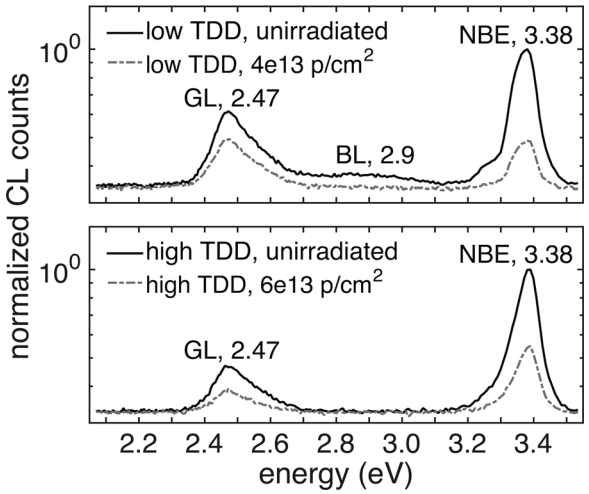

FIG. 4. CL spectra before and after irradiation for low and high TDD materials, normalized to the NBE peaks of the unirradiated samples.

C. DLOS, SSPC, and LCV analysis

Deep level optical spectroscopy (DLOS),[31] steady-state photocapacitance (SSPC), and lighted capacitance-voltage (LCV)[32] were used to identify emergent or ascendant defect states that could be responsible for the observed reduction in the hole diffusion length (L_h) following proton irradiation. DLOS measures the optical deep level energy (E_o) relative to the majority carrier band edge (the conduction band in this case), while SSPC and LCV measure the relative and absolute changes, respectively, in the deep level carrier concentration (N_t). DLOS is a differential photocapacitance technique that uses monochromatic, sub-bandgap energy photons to measure the deep level optical cross-section (σ^o), which is defined as the optical emission rate at a given photon energy ($h\nu$) normalized to the incident photon flux. DLOS and SSPC measurements were performed at room temperature using a Xe arc lamp source filtered through a 1/4 m monochromator with mode-sorting filters to achieve monochromatic illumination from 1.20 to 3.50 eV at a photon flux of $10^{16}\,cm^{-2}\,s^{-1}$ that was held constant by adjusting the monochromator slit width. The deep level σ^o can be thought of as the optical absorbance per unit defect, and fitting the line-shape of σ^o to an appropriate model[33] determines E_o and the Franck-Condon energy (d_{FC}). Typical uncertainty in fitted values of E_o and d_{FC} from our dataset is estimated to be 0.05 eV, and so, E_o and d_{FC}, are rounded to this energy increment. All reported defect energy levels are

optical levels, E_o, rather than thermal levels, E_t, where $E_o = E_t + d_{FC}$. SSPC measures $\Delta C/C_0$, where ΔC is the magnitude of the photocapacitance and C_0 is the equilibrium diode capacitance in the dark. When $N_t \ll N_d$, i.e., $\Delta C/C_0 < 0.1$ and $N_t = 2N_d\Delta C/C_0$. This condition held for some but not all of the observed defects. LCV was used to measure absolute N_t for defect sates with $\Delta C/C_0 > 0.1$. For LCV measurements, *C-V* characteristics were collected using monochromatic illumination to optically depopulate specific deep levels, and their N_t was measured as the change in net space-charge density. The uncertainty of LCV measurements was estimated to be ~10% based on this method of differencing differentiated *C-V* data because both mathematical operations add noise.

Figure 5 shows the DLOS spectra before and after irradiation, where the symbols are the experimental data and the lines are a least-squares fit to the model. The spectra were offset for clarity, and it is important to note that the magnitude of the DLOS spectra does not indicate N_t. For the unirradiated condition of the low TDD epilayer, three deep levels are observed at 2.00 ($d_{FC} = 0.40$ eV), 2.90 ($d_{FC} = 0.45$ eV), and 3.30 eV ($d_{FC} = 0$ eV) below the conduction band minimum (E_c), and a characteristic saturation in the DLOS spectrum is observed at the GaN bandgap energy of 3.4 eV. A similar DLOS spectrum is observed for the as-grown, high TDD sample, except that a deep level at E_c – 3.00 eV ($d_{FC} = 0.60$ eV) appears rather than the E_c – 2.90 eV level. The DLOS spectra for the irradiated condition for both low and high TDD samples are nearly identical, showing three deep levels at E_c – 1.90 ($d_{FC} = 1.40$ eV), 3.00 ($d_{FC} = 0.60$ eV), and 3.30 eV ($d_{FC} = 0$ eV). Constancy of the E_c – 3.00 and E_c – 3.30 eV deep level line-shapes after irradiation indicates that their respective defect microstructure did not change. The fact that the E_c – 2.90 eV deep level spectrum for the as-grown, low TDD sample is supplanted by the E_c – 3.00 eV deep level suggests that the former is related to an extrinsic defect and becomes superimposed by introduction of a native defect after irradiation. The E_o and d_{FC} values for the E_c – 2.90 eV and E_c – 3.00 eV deep levels are similar to those

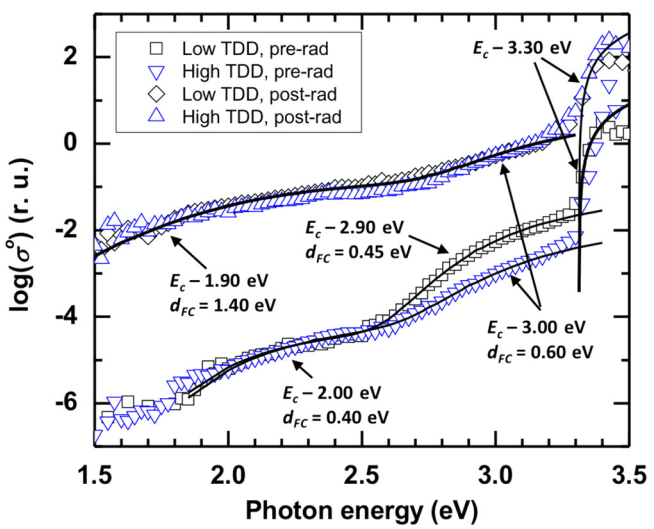

FIG. 5. DLOS spectra before and after irradiation for a low TDD material and a high TDD material. Broadening of the irradiated spectrum between 1.50 and 2.50 eV indicates the introduction of new defect states.

previously ascribed to defects related to carbon[34] and the gallium vacancy (V_{Ga}),[10] so it is reasonable to ascribe the E_c – 2.90 eV level as carbon-related and the E_c – 3.00 eV level as V_{Ga}-related. There is significant broadening for the DLOS spectra between 1.50 and 2.50 eV with irradiation. The large difference in d_{FC} values for the E_c – 1.90 eV and E_c – 2.00 eV deep levels suggests that the former originates from a new defect state that emerges with irradiation, possibly related to Ga_i, as suggested by our EBIC observations and calculations that find that Ga_i forms a deep state with very large lattice relaxation.[35]

The SSPC spectra in Fig. 6 show $\Delta C/C_0$ before and after irradiation for the low and high TDD epilayers to indicate which deep level concentrations changed significantly. SSPC shows the cumulative photocapacitance, which is apportioned among individual deep levels by the change in $\Delta C/C_0$ magnitude over the spectral region for which one dominates. For example, for the irradiated low TDD epilayer in Fig. 6(a), the increase in $\Delta C/C_0$ up to 0.10 between $h\nu = 1.20$ and 2.55 eV corresponds to the introduction of the E_c – 1.90 eV level, the additional increase in $\Delta C/C_0 = 0.19$ between $h\nu = 2.60$ and 3.275 eV corresponds to the E_c – 3.00 eV level, and the additional increase in $\Delta C/C_0 = 0.07$ between $h\nu = 3.30$ and 3.40 eV corresponds to the E_c – 3.30 eV level. Figure 6(a) shows that the only significant increase in $\Delta C/C_0$ with irradiation for the low TDD sample was due to the introduction of the E_c – 1.90 eV deep level. This observation raises the question as to why the DLOS spectra for the low TDD sample between $h\nu = 2.60$ and 3.275 eV broaden with irradiation if there was not significant introduction of defects forming deep levels in this energy range. A possible scenario is that the concentration of V_{Ga}-related defects introduced by irradiation was small relative to the concentration of carbon-related E_c – 3.00 eV deep level defects yet still sufficient to superimpose a broader onset onto the post-irradiation DLOS line-shape. Figure 6(b) shows pre- and post-irradiation the SSPC spectra for the high TDD epilayer, where again the largest increase in $\Delta C/C_0$ corresponded to the introduction of the E_c – 1.90 eV deep level, but $\Delta C/C_0$ of the E_c – 3.00 and E_c – 3.30 eV deep levels increased as well.

The trends of N_t vs. TDD and change in N_t with irradiation were quantified using SSPC or LCV (data not shown), and the results are given in Table I. From Fig. 6, the $\Delta C/C_0$ values for the E_c – 2.00 eV level for both high and low TDD and Ec – 1.90 eV defect for the high TDD sample prior to irradiation were small enough so that SSPC was used to calculate N_t directly, as described above. LCV was used to measure N_t for the remaining deep levels because their corresponding $\Delta C/C_0$ values were greater than 0.1. Considering first the N_t data for the as-grown condition, the only large discrepancy between the low and high TDD epilayers is the >7× larger concentration of the E_c – 2.00 eV deep level for the latter. Taking this observation in conjunction with the EBIC data suggests that the E_c – 2.00 eV deep level could be related to threading dislocations and play a role in reducing L_h by acting as a ~mid-gap non-radiative recombination center.

Comparison of the pre- and post-irradiation N_t data confirms the trend from SSPC in that the only large increase in N_t corresponded to the introduction of the E_c – 1.90 eV deep level, which may be due to Ga_i. The emergence of this deep

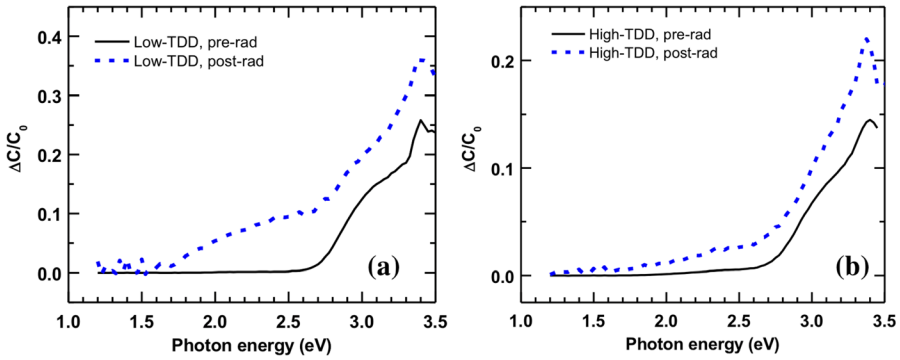

FIG. 6. SSPC spectra before and after irradiation for the low TDD (a) and high TDD (b) epilayers. The large increase in $\Delta C/C_0$ between 1.20 and 2.575 eV for the irradiated condition is the only substantial change for the low TDD sample, indicating that the emergence of the $E_c - 1.90$ eV defect state was the only significant change in the defect concentration. The high TDD epilayer exhibited an increase in $\Delta C/C_0$ for each of the $E_c - 1.90$, $E_c - 3.00$, and $E_c - 3.30$ eV deep levels.

level correlates with degraded L_h in both epilayers, suggesting that the $E_c - 1.90$ eV deep level is also able to trap or scatter holes. The decrease in L_h with respect to proton fluence for the low TDD sample was faster than for the high TDD sample, yet the introduction rate of the $E_c - 1.90$ eV was approximately the same for both epilayers. The discrepancy may suggest that Cottrell atmospheres surrounding dislocation cores getter defects, leading to a lower defect concentration in the regions between dislocations in the high TDD sample, and a more modest decline in L_h. The presence of the $E_c - 1.90$ eV level in the irradiated samples obscures detection of the $E_c - 2.00$ eV level after irradiation.

The $E_c - 2.90/E_c - 3.00$ eV and $E_c - 3.30$ eV deep level defect densities also showed variations with irradiation. The high TDD sample evidenced an increase in N_t with irradiation for the $E_c - 3.00$ eV level, which is attributed to the creation of V_{Ga}-related defects and is consistent with the increase in the GL/NBE peak ratio observed using CL. The apparent reduction in N_t for the $E_c - 2.90/E_c - 3.00$ eV deep levels with irradiation for the low TDD epilayer is likely a result of the uncertainty in the LCV measurement. The increase in N_t for the $E_c - 3.30$ eV deep level with irradiation agrees with a previous study that found a similar defect level at $E_c - 3.25$ eV, also increased with proton bombardment.[36] These observations would suggest that it is associated with a native defect, yet this deep level has often been ascribed to carbon substituting on the nitrogen sub-lattice.[37] A reconciliation of this apparent paradox has been proffered previously, where proton irradiation creates nitrogen vacancies which enables interstitial carbon to impinge onto the substitutional site.[36] It is interesting that the introduction rate for the $E_c - 3.30$ eV deep level is much lower in this study than $\sim 100\ \mathrm{cm}^{-1}$ found by Zhang *et al.* for *n*-type GaN grown by molecular beam epitaxy[36] despite using similar proton energies (i.e., similar non-ionizing energy loss). This difference suggests that the introduction of at least some point defects by protons in GaN can vary based on the crystal growth method.

TABLE I. Deep level defect concentration for the high and low TDD samples before and after irradiation and the associated defect introduction rates.

E_o (eV)	Low TDD N_t (cm^{-3})	Introduction Rate (cm^{-1})	High TDD N_t (cm^{-3})	Introduction rate (cm^{-1})
Pre-irradiation				
2.00	4.3×10^{13}	…	3.1×10^{14}	…
2.90/3.00	6.5×10^{15}	…	6.0×10^{15}	…
3.30	3.2×10^{15}	…	2.4×10^{15}	…
Post-irradiation				
1.90	3.2×10^{15}	80	4.7×10^{15}	78
3.00	5.8×10^{15}	<15	7.7×10^{15}	28
3.30	3.6×10^{15}	10	3.3×10^{15}	15

V. CONCLUSIONS

We examine the effects of 2.5 MeV proton radiation with fluences of $4–6 \times 10^{13}$ protons/cm^2 on the hole diffusion length and point defect characteristics in homoepitaxial (low TDD) and heteroepitaxial (high TDD) n-GaN Schottky diodes. We find that the irradiation lowers the hole diffusion length in GaN by 50%–55%, with a larger reduction in low TDD GaN. In conjunction with this decline in hole transport, we observe several signatures of radiation-induced point defects. A subtle pattern in the EBIC images following irradiation suggests the migration and clustering of point defects at room temperature over a distance of ~500 nm. Our analysis together with prior studies suggests that Ga_i is the likely defect responsible for the observed EBIC contrast following irradiation. CL spectra show GL and BL peaks associated with V_{Ga} and V_{Ga}-related complexes. Irradiation leads to an overall reduction in CL intensity, indicating the introduction of defects that act as non-radiative recombination centers. DLOS measurements identify defect levels associated with V_{Ga}, V_{Ga}-related complexes, and C and reveal the emergence of a level at E_c–1.9 eV following irradiation, which could be related to Ga_i. SSPC and LCV confirm the introduction of the E_c–1.9 eV level as the most prominent effect of the irradiation in both high and low TDD samples.

ACKNOWLEDGMENTS

This work was supported by Sandia's Laboratory-Directed Research and Development program. Sandia National Laboratories is a multimission laboratory managed and operated by the National Technology and Engineering Solutions of Sandia, LLC., a wholly owned subsidiary of Honeywell International, Inc., for the U.S. Department of Energy's National Nuclear Security Administration under Contract DE-NA-0003525.

[1]D. F. Storm, M. T. Hardy, D. S. Katzer, N. Nepal, B. P. Downey, D. J. Meyer, T. O. McConkie, L. Zhou, and D. J. Smith, "Critical issues for homoepitaxial GaN growth by molecular beam epitaxy on hydride vapor-phase epitaxy-grown GaN substrates," J. Cryst. Growth **456**, 121–132 (2016).

[2]B. J. Baliga, "Power semiconductor device figure of merit for high-frequency applications," IEEE Electron Device Lett. **10**(10), 455–457 (1989).
[3]B. J. Baliga, "Gallium nitride devices for power electronic applications," Semicond. Sci. Technol. **28**, 074011 (2013).
[4]S. J. Pearton, F. Ren, E. Patrick, M. E. Law, and A. Y. Polyakov, "Review-ionizing radiation damage effects on GaN devices," ECS J. Solid State Sci. Technol. **5**(2), Q35–Q60 (2016).
[5]K. Motoki, T. Okahisa, N. Matsumoto, M. Matsushima, H. Kimura, H. Kasai, K. Takemoto, K. Uematsu, T. Hirano, M. Nakayama, S. Nakahata, M. Ueno, D. Hara, Y. Kumagai, A. Koukitu, and H. Seki, "Preparation of large freestanding GaN substrates by hydride vapor phase epitaxy using GaAs as a starting substrate," Jpn. J. Appl. Phys., Part 2 **40**(2B), L140–L143 (2001).
[6]K. Motoki, T. Okahisa, R. Hirota, S. Nakahata, K. Uematsu, and N. Matsumoto, "Dislocation reduction in GaN crystal by advanced-DEEP," J. Cryst. Growth **305**(2), 377–383 (2007).
[7]K. Fujito, S. Kubo, H. Nagaoka, T. Mochizuki, H. Namita, and S. Nagao, "Bulk GaN crystals grown by HVPE," J. Cryst. Growth **311**, 3011–3014 (2009).
[8]S. Pearton, R. Deist, A. Y. Polyakov, F. Ren, L. Liu, and J. Kim, "Radiation damage in GaN-based materials and devices," in *Advanced Energy Materials*, edited by A. Tiwari and S. Valyukh (John Wiley & Sons, Inc., Hoboken, NJ, 2014), pp. 345–387.
[9]A. Y. Polyakov, A. S. Usikov, B. Theys, N. B. Smirnov, A. V. Govorkov, F. Jomard, N. M. Shmidt, and W. V. Lundin, "Effects of proton implantation on electrical and recombination properties of n-GaN," Solid-State Electron. **44**, 1971–1983 (2000).
[10]A. Castaldini, A. Cavallini, L. Polenta, and G. Salviati, "Recombination properties of defects in gallium nitride," Solid State Phenom. **78–79**, 95–102 (2001).
[11]A. Pinos, S. Marcinkevicius, M. Usman, and A. Hallen, "Time-resolved luminescence studies of proton-implanted GaN," Appl. Phys. Lett. **95**, 112108 (2009).
[12]A. Y. Polyakov, N. B. Smirnov, A. V. Govorkov, S. J. Pearton, and J. M. Zavada, "Proton implantation effects on electrical and luminescent properties of p-GaN," J. Appl. Phys. **94**(5), 3069–3074 (2003).
[13]K. C. Collins, M. P. King, J. R. Dickerson, G. Vizkelethy, A. M. Armstrong, A. J. Fischer, A. A. Allerman, R. J. Kaplar, O. Aktas, C. Kizilyalli, A. A. Talin, and F. Leonard, "Imaging the impact of proton irradiation on edge terminations in vertical GaN PIN diodes," IEEE Electron Device Lett. **38**(7), 945–948 (2017).
[14]E. B. Yakimov, "What is the real value of diffusion length in GaN?," J. Alloys Compd. **627**, 344–351 (2015).
[15]D. K. Schroder, *Semiconductor Material and Device Characterization*, 3rd ed. (Wiley-Interscience, Hoboken, NJ, 2006).
[16]D. Drouin, A. R. J. D. Couture, X. Tastet, V. Aimez, and R. Gauvin, "CASINO V2.42-A fast and easy-to-use modeling tool for scanning electron microscopy and microanalysis users," Scanning **29**(3), 92–101 (2007).
[17]Z. Z. Bandic, P. M. Bridger, E. C. Piquette, and T. C. McGill, "The values of minority carrier diffusion lengths and lifetimes in GaN and their implications for bipolar devices," Solid-State Electron. **44**, 221–228 (2000).
[18]L. Chernyak, A. Osinsky, G. Nootz, A. Schulte, J. Jasinski, M. Benamara, Z. Liliental-Weber, D. C. Look, and R. J. Molnar, "Electron beam and optical depth profiling of quasibulk GaN," Appl. Phys. Lett. **77**(17), 2695–2697 (2000).
[19]K. Kumakura, T. Makimoto, N. Kobayashi, T. Hashizume, T. Fukui, and H. Hasegawa, "Minority carrier diffusion length in GaN: Dislocation density and doping concentration dependence," Appl. Phys. Lett. **86**, 052105 (2005).
[20]E. B. Yakimov, S. S. Borisov, and S. I. Zaitsev, "EBIC measurements of small diffusion length in semiconductor structures," Semiconductors **41**(4), 411–413 (2007).
[21]E. B. Yakimov, P. S. Vergeles, A. Y. Polyakov, N. B. Smirnov, A. V. Govorkov, I.-H. Lee, C. R. Lee, and S. J. Pearton, "Donor nonuniformity in undoped and Si doped n-GaN prepared by epitaxial lateral overgrowth," Appl. Phys. Lett. **92**, 042118 (2008).
[22]A. Y. Polyakov, N. B. Smirnov, E. B. Yakimov, A. S. Usikov, H. Helava, K. D. Shcherbachev, A. V. Govorkov, Y. N. Makarov, and I.-H. Lee, "Electrical, optical and structural properties of GaN films prepared by hydride vapor phase epitaxy," J. Alloys Compd. **617**, 200–206 (2014).
[23]J. H. Warner, S. R. Messenger, R. J. Walters, G. P. Summers, M. J. Romero, and E. A. Burke, "Displacement damage evolution in GaAs following electron, proton and silicon ion irradiation," IEEE Trans. Nucl. Sci. **54**(6), 1961–1968 (2007).
[24]S. I. Maximenko, S. R. Messenger, C. D. Cress, J. A. Freitas, Jr., and R. J. Walters, "Application of CL/EBIC-SEM techniques for characterization of radiation effects in multijunction solar cells," IEEE Trans. Nucl. Sci. **57**(6), 3095–3100 (2010).
[25]J. F. Ziegler, M. D. Ziegler, and J. P. Biersack, "SRIM-The stopping and range of ions in matter (2010)," Nucl. Instrum. Methods B **268**(11–12), 1818–1823 (2010).
[26]K. H. Chow, G. D. Watkins, A. Usui, and M. Mizuta, "Detection of interstitial Ga in GaN," Phys. Rev. Lett. **85**(13), 2761–2764 (2000).
[27]S. Limpijumnong and C. G. Van de Walle, "Diffusivity of native defects in GaN," Phys. Rev. B **69**, 035207 (2004).
[28]O. Ambacher, F. Freudenberg, R. Dimitrov, H. Angerer, and M. Stutzmann, "Nitrogen effusion and self-diffusion in $Ga_{14}N/Ga_{15}N$ isotope heterostructures," Jpn. J. Appl. Phys., Part 1 **37**(5A), 2416–2421 (1998).
[29]N. Faleev, H. Temkin, I. Ahmad, M. Holtz, and Y. Melnik, "Depth dependence of defect density and stress in GaN grown on SiC," J. Appl. Phys. **98**, 123508 (2005).
[30]M. A. Reshchikov and H. Morkoc, "Luminescence properties of defects in GaN," J. Appl. Phys. **97**, 061301 (2005).
[31]A. Chantre, G. Vincent, and D. Bois, "Deep-level optical spectroscopy in GaAs," Phys. Rev. B **23**(10), 5335–5359 (1981).
[32]A. Armstrong, A. R. Arehart, and S. A. Ringel, "A method to determine deep level profiles in highly compensated, wide band gap semiconductors," J. Appl. Phys. **97**, 083529 (2005).
[33]R. Passler, "Photoionization cross-section for a deep trap contributing to current collapse in GaN field-effect transistors," J. Appl. Phys. **96**(1), 715–722 (2004).
[34]T. Ogino and A. Masaharu, "Mechanism of yellow luminescence in GaN," Jpn. J. Appl. Phys., Part 1 **19**(12), 2395–2405 (1980).
[35]C. G. Van de Walle and J. Neugebauer, "First-principles calculations for defects and impurities: Applications to III-nitrides," J. Appl. Phys. **95**(8), 3851–3879 (2004).
[36]Z. Zhang, A. R. Arehart, E. Cinkilic, J. Chen, E. X. Zhang, D. M. Fleetwood, R. D. Schrimpf, B. McSkimming, J. S. Speck, and S. A. Ringel, "Impact of proton irradiation on deep level states in n-GaN," Appl. Phys. Lett. **103**, 042102 (2013).
[37]A. Armstrong, C. Poblenz, D. S. Green, U. K. Mishra, J. S. Speck, and S. A. Ringel, "Impact of substrate temperature on the incorporation of carbon-related defects and mechanism for semi-insulating behavior in grown by molecular beam epitaxy," Appl. Phys. Lett. **88**, 082114 (2006).